Flow Visualization over the Blunted Edge Airfoil to Reducing the Drag by using Water Flow Channel Method and Wind Tunnel Technique

N. Vairamuthu
Assistant Professor
Dept of AERO- PITS

D. Shalini
Dept of AERO- PITS

M. Sivaranjani
Dept of AERO- PITS

Abstract:- **This paper expresses the concept of modifying the trailing edge of an airfoil by blunted trailing edge configuration. The purpose of designing the modification of airfoil is helps to reduce the drag. The velocity field around the original airfoil and the new airfoil is measured by wind tunnel technique and water flow channel method then comparing the data with each other. After cutting the end of sharpened trailing edge can decreases the vortex formation.**

INTRODUCTION

Airfoils with thickened edges are used in subsonic flow to resolve many of the problems encountered in the conventional airfoils.

In the conventional airfoils, the trailing edge ends to a sharp point. However, for certain applications (e.g., a wing in high attack angles), an airfoil with a thick trailing edge is required. The gradual reduction of sharpness at the downstream of the maximum thickness section of an airfoil creates a strong positive pressure gradient at its low-pressure side, leading to an untimely flow separation. This positive pressure gradient can be somewhat reduced using a thickened edge. Thus, the recovered pressure can be partially transferred to the separation region produced by the airfoil. Improving the aerodynamic performance of airfoils with thickened edges would require certain drag-reduction. Baker and Dam (numerically and experimentally studied the FB-3500-1750 airfoil with blunt trailing-edge and used certain instruments to reduce the drag and increase the lift for improving the performance of this airfoil. They used a pyramidal balance for the measurement of the lift and drag at Davis aeronautical wind tunnel. To reduce drag, they implemented two splitter plates as well as open and moderate cavities. Their results showed that using the splitter plates could reduce drag by up to 50%. Although a base cavity reduced drag by up to 25%, it also introduced drastic fluctuations in lift. Using a Moderate cavity not only improved the drag-reducing performance of the splitter plate, but also limited the unsteady vortex shedding. It conducted a numerical study on the sinusoidal edge effect in a flow stopping airfoil-like body with a thick edge to determine how it affected the aerodynamic characteristics of this body. They examined the effect of the sinusoidal edge wavelength on drag coefficient, vortex shedding, and frequency. Their results showed that using a specific wavelength would reduce drag more than 30% as compared with the drag produced by a smooth-edged airfoil. In this case, the smaller separation region resulting from reduced drag would lead to a further reduction in the frequency of oscillations inside the separation region as well as increased flow vorticity.

By measuring pressure on the upper surface of an airfoil and implementing the particle image velocity technique, (studied the flow behavior over a two- dimensional bluff body combined to a base cavity with various shapes. For this purpose, they used four types of cavities. Their experiments with the moderate cavity showed that two rotational regions adjacent to the base cavity were created. Moreover, dramatic variations were observed in the length of the recirculation region as well as the mean flow field in the presence of the base cavity. It conducted theoretical and experimental studies on the NACA0012 airfoil with a thick edge They produced the thick-edged airfoil by cutting off the trailing edge of the airfoil at the following distances: 5, 10, and 15% of the chord length as measured from the end of the airfoil.

WINDTUNNEL TESTSETUP

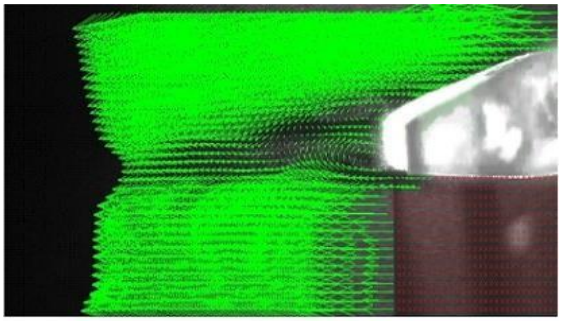

(a) t = 0

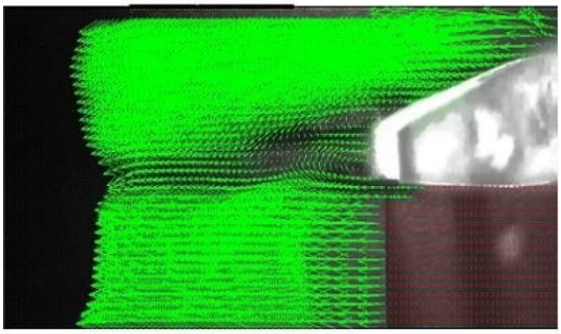

(b) t = 0.0056s

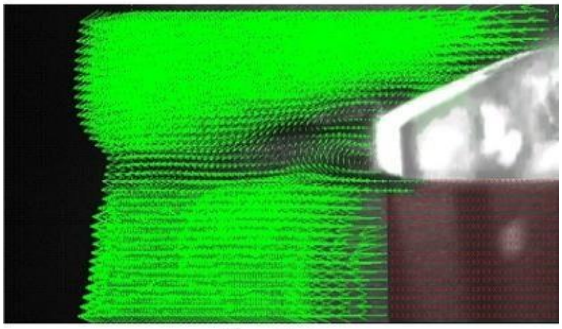

(c) t = 0.0112s

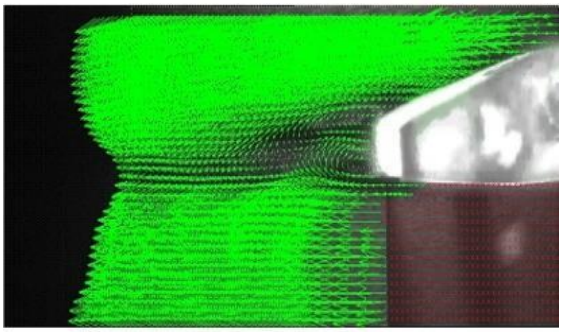

(d) t = 0.0168s

They calculated the induced lift and drag forces in a wind tunnel at angles between 0° and 20° and *Re* = 400,000.
The results showed that lift and drag both increased as a result of increasing the trailing edge thickness. They used the hot wire apparatus as well as flow detection techniques to conduct their experiments. Their results revealed using trapezoidal prismatic blocks somewhat weakened the Carman vortices formed at the back of the airfoil. However, pressure distribution measurements showed that drag was reduced by a mere 3–4%. It was studied the aerodynamic effects of two types of cavity on the NACA0018 airfoil. By flow visualization experiments, they observed vortexes instabilities which produce oscillating force cavity on the stability of the trapped vortex.

WIND TUNNEL RESULTS FOR THE THICK BLUNT TRAILING-EDGE AIRFOIL

Keeping Reynolds number and attack angle constant (*Re* = 2150 and attack angle = 5°), the PIV tests are performed again for the thick blunt trailing-edge airfoil. Figure 5 shows the instantaneous velocity vectors obtained for this case. The time frame between two consecutive images is 0.0056 s. As seen, no separation occurs on the airfoil surface, and only two vortices are formed behind thick blunt trailing edge. In fact, using this thick blunt trailing-edge airfoil causes the location of the separation region to move from the airfoil surface to the back of the airfoil. No further vortex shedding is observed at this point and, as said before, only two vortices are formed at the upper and lower parts of the airfoil with counter clockwise and clockwise rotations respectively. It location, but move at a specific frequency along the flow as explained here. First, a counter clockwise vortex is separated from the upper shear layer and starts moving with the flow before disappearing towards the end of the separation zone. A second vortex (rotating clockwise) is immediately separated from the lower shear layer, again moving with the flow until it vanishes. This is periodically repeated at a specific frequency. Figure shows the instantaneous velocity vectors for a vortex shedding time period at *Re* = 3220 and attack angle of 5°. The time between two consecutive images is 0.009 s. As observed, in the first two images, the upper vortex, rotating counter clockwise, is moving in the same direction as the free stream. In the third image, this vortex is disappearing and a second vortex is being formed at the lower part, rotating in a clockwise direction. In the fourth image, the lower vortex is fully formed and is moving in the direction of the free flow. In the fifth image, this vortex is also disappearing and a third upper vortex is being formed. Finally, the last image shows that the lower vortex fully vanishes and the upper vortex is fully and, thus, the cycle is completed.

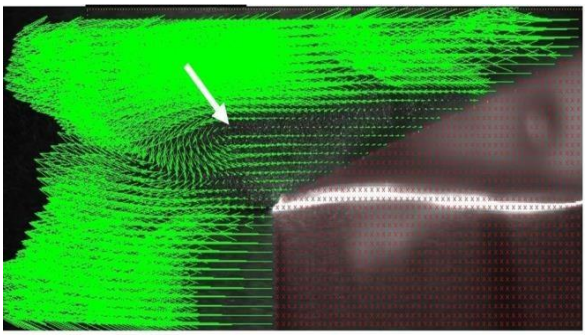

(a) t = 0.0035s

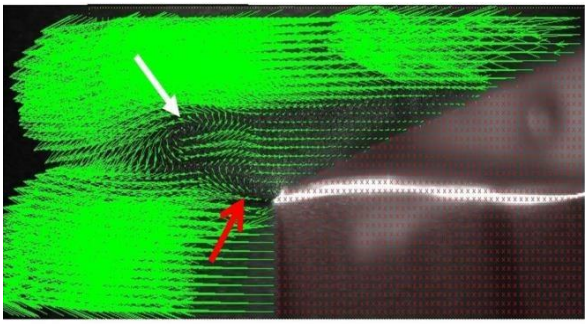

(b) t = 0.0105s

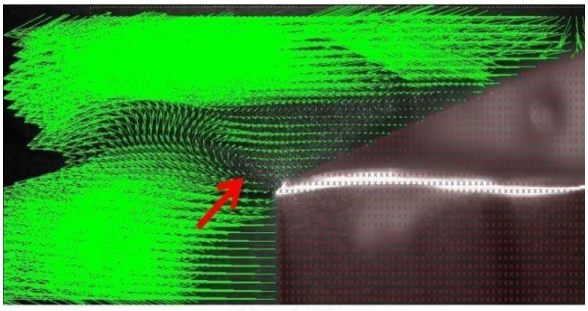

(c) t = 0.0175s

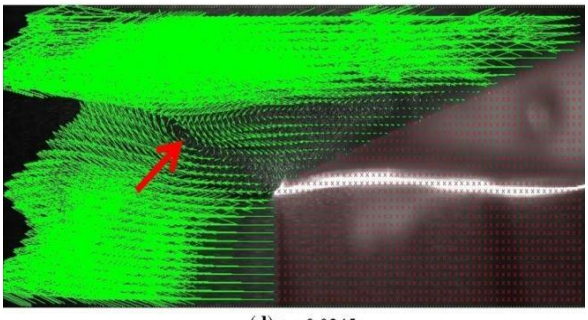

(d) t = 0.0245s

VELOCITY DISTRIBUTIONS BEHIND THE TRAILING EDGE

In five sections at the back of the airfoil trailing edge has been specified along which velocity distributions are plotted. These five sections are located at 10, 20, 30, 40, and 50% of the chord length (5 cm) from the trailing edge. Figure shows the mean velocity distributions along the five specified sections at the attack angle of 5° and the Reynolds number of 3070. The mean velocity distributions are averaged by taking the mean values for several vortex shedding periods. The coordinate origin coincides with the upper point of the diagram. As can be observed, at the initial sections (10 and 20% of the chord), there are two minimum points in the diagram.

These points appear due to the formation of two vortices within the separation region. These vortices are the same as those formed during the vortex shedding (in the previous section) which occurred near the upper and lower shear layers. As we move further from the trailing edge, the effects of these two vortices diminish and the two minimum points are consequently merged. As the distance of the section from the end point is further increased, this recirculation region gradually vanishes. The close region between the black line (1m/s) there is a maximum point above the airfoil. As shown in this figure, the flow velocity increases up to a certain point and then decreases. As can be seen, such a point does not exist under the airfoil. As the flow is separated on the airfoil, the free flow above the shear level is accelerated and flow velocity at the upper shear layer increases.

Therefore, the maximum point is due to this acceleration in the proximity of the upper shear layer. This phenomenon can be explained as follows: the flow first accelerates while passing over the upper airfoil surface before encountering a positive pressure gradient.

However, upon flow separation, full pressure recovery does not occur. Therefore, we expect the flow velocity in the upper part of the separated region to exceed that of the free air flow velocity. Figure shows the flow velocity profiles at various sections of the thick blunt trailing edge airfoil for the Reynolds number of 2150 and attack angle of 5°. The chord length for this airfoil is 3.5 cm. As seen, the maximum velocity point that exists in Fig. no longer appears and the flow velocity remains constant upon reaching its maximum value. As was mentioned above, the flow over the thick blunt trailing edge airfoil, positioned at a 5° angle of attack, does not undergo separation and this is why a maximum velocity point.

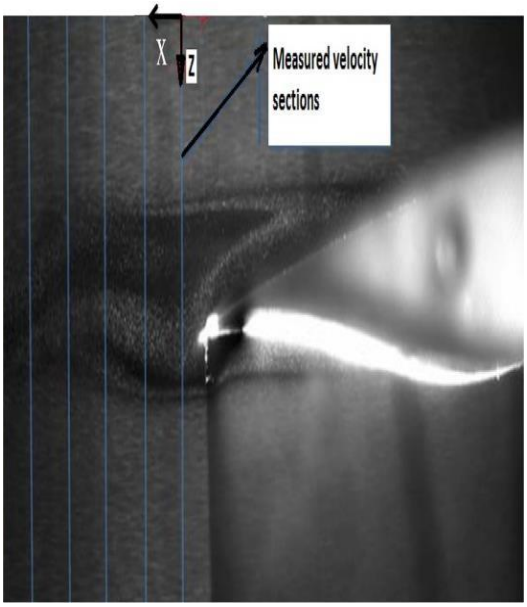

FIG. 5.1 SECTIONS BEHIND THE AIRFOIL FOR MEASUREMENT OF FLOW VELOCITY DISTRIBUTION.

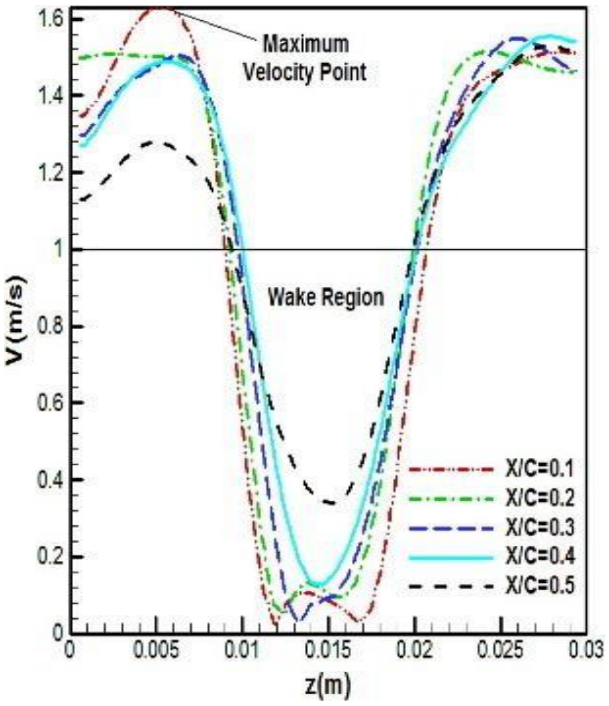

FIG. 5.2 VELOCITY DISTRIBUTION AT VARIOUS SECTIONS OF THE ORIGINAL AIRFOIL AT A 5° ANGLE OF ATTACK AND *U* = 1 M/S

Figure 5.1 shows the instantaneous velocity vectors for the thick blunt trailing-edge airfoil connected to a base cavity (angle of attack = 5° and *Re* = 2150). Similar to the case without base cavity, no separation occurs here either. It is obviously observed here that the separation region behind the airfoil has changed its shape into a pointed triangle, and that the separation region is much smaller than that observed when no cavity was used. Due to the use of dark colored blades, the flow inside the cavity could not be observed. The reason why dark blades are used is that they prevent light reflection which would distort the images. As the Reynolds *U* = 1.5 m/s, and attack angle = 5 number increases, the momentum also increases, leading to the instability of these vortices. Thus, the vortices exit the cavity and become observable. Although these vortices are much smaller than those observed when no cavity is used, they are, nevertheless, observable and move periodically along the flow line. Figure 5.2 shows the instantaneous velocities for one period of oscillation. In the third image, the vortex has fully separated from the cavity edge and is moving along the flow line. At the same time, a second vortex (rotating in a clockwise sense) is formed and separated from the lower edge. The Riso airfoil with a chord length of 5 cm and span of 8 cm is placed inside the wind tunnel with the blockage ratio of 12.5%. Maximum thickness of the airfoil is 1 cm. To produce a thick blunt trailing-edge airfoil, the trailing edge of the Riso airfoil is cutoff at a distance of 30% of chord length from its trailing edge. In the last stage, two 2 mm plates are connected to the end of the thick blunt trailing-edge airfoil to form a base cavity behind the airfoil. Figure 2 shows the mentioned profiles used in this study, including: (1) the Riso airfoil, (2) the thick blunt trailing-edge airfoil, and (3) the thick blunt trailing-edge airfoil with a base cavity profile. In this study, the original airfoil is placed inside the wind tunnel and flow patterns behind the model are measured at different Reynolds numbers and different angles of attack via wind tunnel technique. Then, the same process is repeated for the thick blunt trailing-edge airfoil with and without the base cavity, respectively. Since the flow is laminar, the time scale of the flow pattern is the cord length divided by the flow free stream.

A Riso airfoil, b thick blunt trailing-edge airfoil, and c thick blunt trailing-edge airfoil with a base cavity profile velocity. In this study, the flow velocity is 1–3 m/s and the cord length is 50 mm, so the time scale is 0.05 s which is one order of magnitude larger than the imaging time sequence.

IMAGE PROCESSING

In this research, velocity vectors are obtained by the PIV lab1.32 software in which FFT algorithm is used for image processing. This algorithm has a high accuracy, especially for flow fields with rotating and stretching movements as well as pure translation. In fact, FFT is a multi-stage method in which the interrogation window is reproduced at each stage to be capable of capturing rotating and stretching.

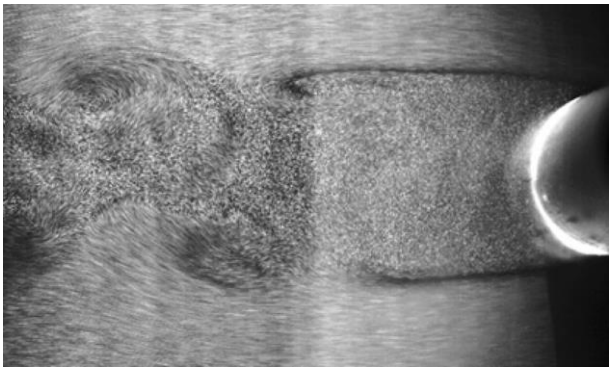

Uncertainty in PIV method can be divided into two main parts: first, the general errors due to tracer particles lag and their not completely following from the flow pattern, and the second one, the error of image processing. the separation region length would decrease in the absence of a base cavity. The reason is that: at low *Re*, the vortices are sucked into the base cavity and are thus stabilized. As *Re* increases, the flow momentum used. In each stage, 50% overlap is applied; thus, the By measuring pressure on the upper surface of an airfoil and implementing the particle image velocity technique, (studied the flow behavior over a two-dimensional bluff body combined to a base cavity with various shapes. For this purpose, they used four types of cavities. Their experiments with the moderate cavity showed that two rotational regions adjacent to the base cavity were created. Moreover, dramatic variations were observed in the length of the recirculation region as well as the mean flow field in the presence of the base cavity. It

conducted theoretical and experimental studies on the NACA0012 airfoil with a thick edge. They produced the thick-edged airfoil by cutting off the trailing edge of the airfoil at the following distances: 5, 10, and 15% of the chord length as measured from the end of the airfoil. They calculated the induced lift and drag forces in a wind tunnel at angles between 0° and 20°.

SIZE OF SEPARATIONREGION

Figure shows the size of the separation region for the thick blunt trailing-edge airfoil with and without base cavity at attack angle of 5° and various Reynolds numbers. As observed, the size of the separation region was smaller in the case with the base cavity than that without it. This can be indicative of the positive effect of using a base cavity. However, another noteworthy point is that in the presence of a base cavity, the separation region length increases

UNCERTAINTY ANDVALIDATION

Uncertainty in PIV method can be divided into two main parts: first, the general errors due to tracer particles lag and their not completely following from the flow pattern, and the second one, the error of image processing.
Re = 400,000.

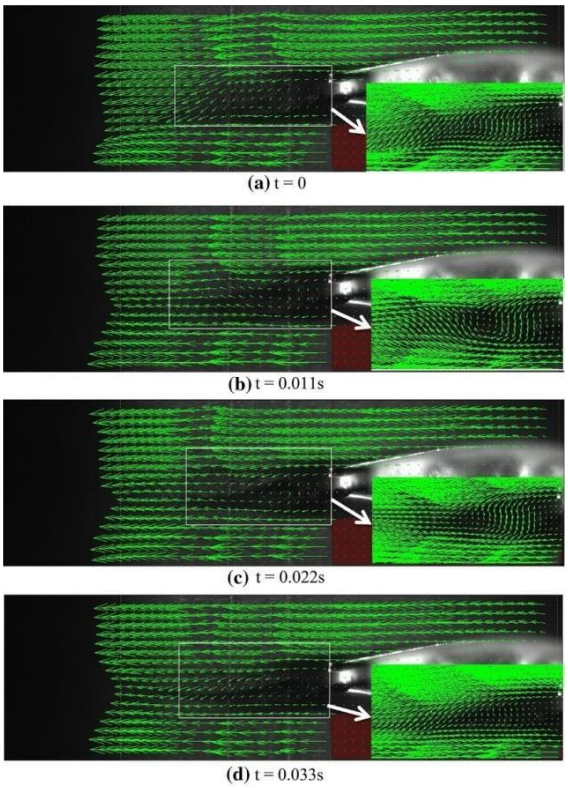

FIG:6 INSTANTANEOUS VELOCITY VECTORS FOR FLOW OVER THE THICK BLUNT TRAILING-EDGE AIRFOIL WITH BASE CAVITY AT VARIOUS INSTANCES FOR ANGLE OF ATTACK = 5° FOR *RE* = 2150 AND *U* = 1 M/S

with increasing Reynolds number; whereas the separation region length would decrease in the absence of a base cavity. The reason is that: at low *Re*, the vortices are sucked into the base cavity and are thus stabilized. As *Re* increases, the flow momentum used. In each stage, 50% overlap is applied; thus, the computation error is 1 pixel. By considering the blockage length of the model for image calibration,

CONCLUSION

In this study, the PIV technique was continuously used to study the flow velocity field around three types of airfoils, including an original thick airfoil with sharp trailing edge, a thick blunt trailing-edge airfoil created from cutting off the original airfoil, and the thick blunt trailing-edge airfoil with a base cavity.

REFERENCES

[1] Aravind A, Al-Garni A (2009) Experimental investigation of the effect of base cavities on the base pressure and wake of two-dimensional bluff body. Adv Fluid Mech Heat Mass Transf 10:366–373

[2] Baker J, Dam C (2008) Drag reduction of blunt trailing-edge airfoils. Bluff Bodies Aerodyn Appl, Milano, pp 20–24 BourgoyneD, CeccioS,DowlingD, Jessup S,ParkJ,BrewerW,PankajakshanR(2000)Hydrofoi lturbulentboundarylayerseparation at high Reynolds number. In: Proceedings of the 23rd symposium on naval hydrodynamics, Val de Reuil, France.

[3] Cai J, Chng T, Tsia H (2008) On vortical flows shedding from a bluff body with a wavy trailing edge. Phys Fluids 20:064102 Cooperman A, McLennan A, Chow R, Baker J, Dam C (2010) Aerodynamic performance of thick blunt trailing edge airfoils.

[4] Donelli R, Iannelli P, Iuliano S, Rosa D (2011) Suction optimization on thick airfoil to trap vortices. Physics and Fluids Unit, Centro Italiano Ricerche Aerospaziali (CIRA), Via Maiorise,Milano, pp 20–24 BourgoyneD,CeccioS,DowlingD,JessupS,ParkJ,Brewer W,PankajakshanR(2000)Hydrofoilturbulentboundarylay erseparation at high Reynolds number. In: Proceedings of the 23rd symposium on naval hydrodynamics, Val de Reuil, France.